

## SIMULATION OF LATERAL SPREADING OF GENTLY SLOPING LIQUEFIED GROUND

Iman VAEZI

*M.Sc., Shahid Beheshti University, Tehran, Iran  
me@liquefaction.ir*

Ali NOORZAD

*Assistant Professor, Shahid Beheshti University, Tehran, Iran  
a\_noorzad@sbu.ac.ir*

**Keywords:** Liquefaction, Lateral Spreading, Finite Element Method, Pastor-Zienkiewicz-Mark III, U-W Formulation of Porous Media, Centrifuge Liquefaction Experiments

### ABSTRACT

This paper is focused on the simulation of the lateral spreading phenomenon and the anticipated maximum surface displacements of sloping ground. An innovative numerical methodology is proposed employing a generalized plasticity model implemented in a finite element code (Chan, 1988) which has been thoroughly validated against VELACS centrifuge liquefaction experiments (Arulanandan and Scott, 1993). The results of numerical analysis compared with experimental measurements indicate that the proposed numerical model has the capability to simulate the lateral spreading phenomenon. Then this model has been used to find out the effect of frequency of input motion on the magnitude of soil displacement. The results demonstrate that the amount of maximum displacement is significantly decreased by increasing the magnitude of frequency.

### INTRODUCTION

The lateral movement of a liquefiable layer on gently slopes is the most visible and devastating type of liquefaction-induced ground failure. Occurrence of liquefaction in sloping ground causes large deformations on ground surface, which may lead to several meters in some cases. Recent earthquakes have shown that this phenomenon causes severe damages to coastal structures, piers of bridges and life-lines, by exerting large lateral forces. Fortunately, there exist methods today which can be used for the design of such structures against lateral spreading (e.g. P-y analysis). However, their accuracy depends greatly on the ability to estimate the anticipated lateral ground displacements and their variation with depth.

### NUMERICAL METHODOLOGY

In this research, a fully coupled two-dimensional dynamic analysis based on effective stress formulation using saturated porous media considering fluid movement has been used to simulate the lateral spreading and evaluate the amount of deformations occurred in liquefiable soils (Zienkiewicz et al., 1999). The governing equations are developed for saturated porous media based on the extension of Biot formulation (Biot, 1955, 1956). The cyclic elastoplastic behavior of soil under earthquake loading is modeled using the generalized plasticity theory composing of a yield surface together with non-associated flow rule proposed by Pastor and Zienkiewicz (Pastor et al., 1990). A fully explicit dynamic finite element method and a fully coupled (u-w) formulation are employed in a computer code to analyze soil displacements and pore water pressures (Taslimian et al., 2012).

Geometry of the problem is modeled in two dimension. The model was first statically analyzed under gravity force and after the steady state, output stresses was considered in he dynamic analysis as insitu stresses. Dynamic analysis was done by time history method and imposing dynamic loads to the model.

## GOVERNING EQUATIONS

In this section dynamic equations governing saturated porous media are explained, then the constitutive model employed in the modelling is illustrated.

### 1. FULLY COUPLED FORMULATION GOVERNING SATURATED POROUS MEDIA

The four governing equations could be expressed as follows:

#### i. Overall equilibrium

$$\sigma_{ij,j} + \rho b_i - \rho \ddot{u}_i - \rho_f \ddot{w}_j = 0 \quad (1)$$

in which  $\sigma_{ij}$  is the total stress tensor,  $b_i$  is the body acceleration,  $u_i$  and  $w_j$  are solid skeleton and relative average fluid acceleration,  $\rho_f$  is the density of fluid and  $\rho$  is the density of total composite defined as:

$$\rho = n\rho_f + (1 - n)\rho_s \quad (2)$$

where  $\rho_s$  is the density of the solid particles and  $n$  is the porosity.

#### ii. Fluid momentum balance

$$-p_{,i} + \rho_f b_i - \rho_f \ddot{u}_i - \rho_f \frac{\dot{w}_i}{n} = \frac{\rho_f g}{k_{ji}} \dot{w}_j \quad (3)$$

$k_{ji}$  indicates the permeability coefficient tensor and equal to  $k\delta_{ij}$  in the isotropic state.  $g$  is the gravity acceleration and  $p$  is the pore pressure tensor.

#### iii. Effective stress

$$\sigma''_{ij} = \sigma_{ij} + \alpha \delta_{ij} p \quad (4)$$

where  $\sigma''_{ij}$  is the modified effective tensor and  $\alpha$  is the Biot's coefficient defined as:

$$\alpha = 1 - \frac{K_T}{K_S} \quad (5)$$

$K_S$  is the bulk modulus of the grains and  $K_T$  is the bulk modulus of the total mixture.

#### iv. Fluid mass conservation

$$\dot{p}/Q + \alpha \dot{\varepsilon}_{ii} + \dot{w}_{i,i} = 0 \quad (6)$$

$$\frac{1}{Q} = \frac{n}{K_f} + \frac{\alpha - n}{K_S} \quad (7)$$

where  $K_f$  is the bulk modulus of the fluid and  $\varepsilon_{ij}$  is the small strain tensor defined as:



$$\varepsilon_{ij} = 0.5 \left( \frac{\partial u_i}{\partial x_j} + \frac{\partial u_j}{\partial x_i} \right) \quad (8)$$

For u-w approximation, equation 6 is integrated in time:

$$p = -Q(\varepsilon_{ii} + w_{i,i}) \quad (9)$$

By inserting the equation 9 into the equation 3:

$$\alpha Q u_{j,ji} + Q w_{j,ji} - \rho_f \ddot{u}_i - \frac{\rho_f}{n} \ddot{w}_i - \frac{\rho_f g}{k_{ij}} \dot{w}_j + \rho_f b_i = 0 \quad (10)$$

Equations 1 and 10 along with relations 4 and 8 form the governing equations. For solving these equation a constitutive relation is required defined as elastic-plastic behavior:

$$d\sigma'' = D d\varepsilon \quad (11)$$

Where D is the tangent modulus.

## 2. CONSTITUTIVE MODEL FOR SAND

The liquefiable sand is modelled using Pastor-Zienkiewicz-Mark III (Pastor et al., 1990; Zienkiewicz et al., 1985; Zienkiewicz et al., 1999). The model is developed to represent the behaviour of sand under cyclic and monotonic loading condition. Both volumetric and deviatoric plastic strains are included in the hardening parameters of the yield surface to consider unloading and reloading paths. Because of the seismic volumetric deformation due to dilatancy is the main reason for the earthquake induced soil liquefaction, the model employed in this research is the most appropriate one for soils susceptible to liquefaction. In the present study, the 12 model constants indicated in Table 1 retain the values that were calibrated on the basis data from element laboratory tests performed on fine Nevada sand at relative density  $D_r=40\%$  and initial effective stress  $p'_0 = 4kPa$  (Chan & Zienkiewicz, 1998).

Table 1. Parameters of Pastor-Zienkiewicz-Mark III

Parameters	Loose sand ( $D_r=40\%$ )
$M_g$	1.15
$M_f$	1.035
$g$	0.45
$f$	0.45
$K_{ev0c}$	770 kPa
$K_{es0c}$	1155 kPa
$0$	4.2
$1$	0.2
$H_0$	600
$H_{uo}$	4000 kPa
$H_u$	2
DM	0
$P'_G$	4 kPa

## NUMERICAL DISCRETIZATION

In this section governing equations are discretized in time and space then demonstrated in matrix form.

### 1. SPATIAL DISCRETIZATION

Interpolated displacement values for solid and fluid are approximated as below:

$$u \cong \sum_{k=1}^n N_k^u \bar{u}_k = N_k^u \bar{u}_k \quad (12)$$

$$w \cong \sum_{k=1}^n N_k^w \bar{w}_k = N_k^w \bar{w}_k \quad (13)$$

$$N_k = N_k(x, y, z) \quad (14)$$

$$\bar{u}_i \equiv \bar{u}_i(t) \quad (15)$$

$$\bar{w}_i \equiv \bar{w}_i(t) \quad (16)$$

Where  $u$  and  $w$  are solid and relative fluid displacement and  $N_k^u$  and  $N_k^w$  are solid and fluid shape functions respectively. Incorporating these relations, equations 1 and 10 are changed into sets of algebraic equations integrated by part as shown below:

$$\int_{\Omega} N_k^{uT} [\sigma_{ij,j} + \rho b_i - \rho \ddot{u}_i - \rho_f \dot{w}_i] d\Omega = 0 \quad (17)$$

$$\int_{\Omega} N_k^{wT} [\alpha Q u_{j,ji} + Q w_{j,ji} - \rho_f \ddot{u}_i - \frac{\rho_f}{n} \dot{w}_i - \frac{\rho_f g}{k_{ji}} \dot{w}_j + \rho_f b_i] d\Omega = 0 \quad (18)$$

Finally in the matrix form:

$$\begin{Bmatrix} M \\ G^T \end{Bmatrix} \begin{Bmatrix} \ddot{u} \\ \dot{w} \end{Bmatrix} + \begin{Bmatrix} C \\ 0 \end{Bmatrix} \begin{Bmatrix} \dot{u} \\ \dot{w} \end{Bmatrix} + \begin{Bmatrix} \int_{\Omega} B^T \sigma d \\ \int_{\Omega} \frac{\partial N^w}{\partial x} p d \end{Bmatrix} = \begin{Bmatrix} f_b + f_{\sigma} \\ f_b' - f_p \end{Bmatrix} \quad (19)$$

$$M = \int_{\Omega} (N^u)^T \rho N^u d \quad (20)$$

$$G = \int_{\Omega} (N^u)^T \rho_f N^w d \quad (21)$$

$$\bar{M} = \int_{\Omega} (N^w)^T \frac{\rho_f}{n} N^w d \quad (22)$$

$$\bar{C} = \int_{\Omega} (N^w)^T \begin{bmatrix} k_{xx} & k_{xy} \\ k_{yx} & k_{yy} \end{bmatrix}^{-1} N^w d\Omega \quad (23)$$

$$C = \alpha M + \beta K_e \quad (24)$$

$$K_e = \int_{\Omega} B^T D_e B d \quad (25)$$

in which  $B$  is the strain matrix,  $D_e$  is the elastic constitutive matrix,  $C$  is the artificial damping matrix (might be Rayleigh type) exerted to the solid phase.  $f_b$ ,  $f_b'$ ,  $f_{\sigma}$  and  $f_p$  are the forces applied from body forces on the total mixture and fluid, external stresses and pressures.

## 2. TIME DISCRETIZATION

Equation 19 is solved by a finite difference method named generalized Newmark time integrating (GNpj)(Newmark, 1959). In the time of  $t_{n+1}$ , unknown values  $u_{n+1}$ ,  $w_{n+1}$  and  $p_{n+1}$  are calculated based upon known values  $u_n$ ,  $w_n$  and  $p_n$  in the time of  $t_n$ . GNpj method is described for solid phase as:

$$\ddot{u}_{n+1} = \ddot{u}_n + \ddot{u}_n \quad (26)$$

$$\dot{u}_{n+1} = \dot{u}_n + \ddot{u}_n \Delta t + \beta_1 \ddot{u}_n \Delta t \quad (27)$$

$$u_{n+1} = u_n + \dot{u}_n \Delta t + \ddot{u}_n \frac{\omega t^2}{2} + \beta_2 \ddot{u}_n \frac{\omega t^2}{2} \quad (28)$$



where  $\beta_1$  and  $\beta_2$  are numerical damping coefficients in the time domain and assumed between 0 and 1. Considering u-w fully explicit formulation these equations are used for both u and w, however  $\beta_2$  should be zero in order to avoid numerical instability.

## NUMERICAL MODELLING

In this section equations governing the problem described in previous sections are solved for dynamic problem with high frequency. Hence, a fully explicit computer code was employed called GLADYS-2E developed by Chan(Chan et al., 1994; Chan et al., 1992) following the work described by (Zienkiewicz & Shiomi, 1984). In order to verify this code, one of the centrifuge experiment namely M2-1 was simulated and the results are illustrated in the next section. Modelling procedure is described in the following:

### 1. MODEL GEOMETRY

The mesh used in modelling is depicted in Figure 1. For modelling boundary conditions, the bottom of the mesh was fixed in both directions; the lateral boundaries were tied to one another in order to enforce the same horizontal and vertical displacements of the two boundaries, as imposed by the laminar box device in the centrifuge experiments. Hence, no stress boundaries were used for the bottom and lateral boundaries. It is assume and apply that drainage only occurs through top boundaries and other boundaries are completely impermeable.

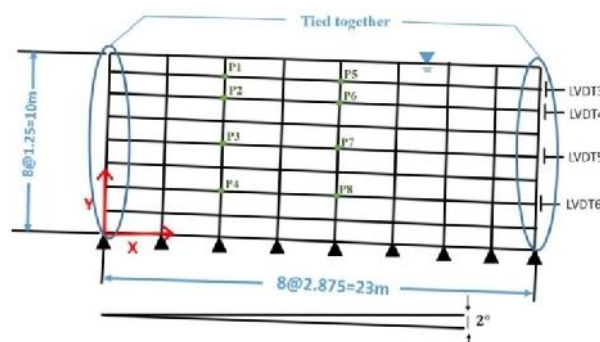


Figure 1. Finite element mesh used for the numerical simulation of centrifuge tests and associated instrumentation for test M2-1(Arulanandan & Scott, 1993)

### 2. MODEL PARAMETERS

Specifications of Nevada sand used in modelling are the same as centrifuge experiment VELACS M2-1 that is given in Table 2. After sensitivity analysis, time step was considered  $\Delta t = 0.0005s$  and Newmark parameters were chosen  $\alpha = 0.5$  and  $\beta = 0$ .

Table 2. Parameters of Nevada sand used in the modelling

Parameters	Dimension	For $D_r=40\%$
Porosity	-	0.42
Permeability coefficient	m/s	$6.60 \times 10^{-5}$
Permeability coefficient For prototype	m/s	$0.33 \times 10^{-2}$
Elastic modulus	kPa	2000
Poison Ratio	-	0.30
Average density	kN/m <sup>3</sup>	19.57
Water density	kN/m <sup>3</sup>	9.80
Biot coefficient ( $\alpha$ )	-	1.00
Solid bulk modulus	GPa	$10^{11}$
Fluid bulk modulus	GPa	1.09

### 3. MODELLING PROCEDURE

Appropriate normal stress and related pore water pressure variation was applied at the top boundary to simulate the gently inclined layer of water existing on top of the sand layer in all tests to ensure that the degree of saturation is one. Static analysis in the form of dynamic relaxation was performed to obtain initial static equilibrium in order to create the equilibrium stress field of the soil with a gently sloping ground surface, and then the dynamic load was applied. Fully coupled analysis was performed for taking into account the interaction between the mechanical behavior and the diffusion process. In the static analysis in order to avoid developing tensile stress and high stress ratio, non-associated elastoplastic Mohr-Coulomb with reduced friction angle was used. Parameters of this model are illustrated in Table 3.

Table 3. Parameters of Mohr-Coulomb model

Parameters	$D_r=40\%$
Elastic modulus	2000 kPa
Poisson ratio	0.4
Axial yield stress	2.49 kPa
Dilatancy angle	$0.66^\circ$
Reduced friction angle	$25^\circ$

The reported horizontal and vertical excitations were imposed as an acceleration time history at the base of the model parallel with inclination. Figure 2 shows the input time history acceleration.

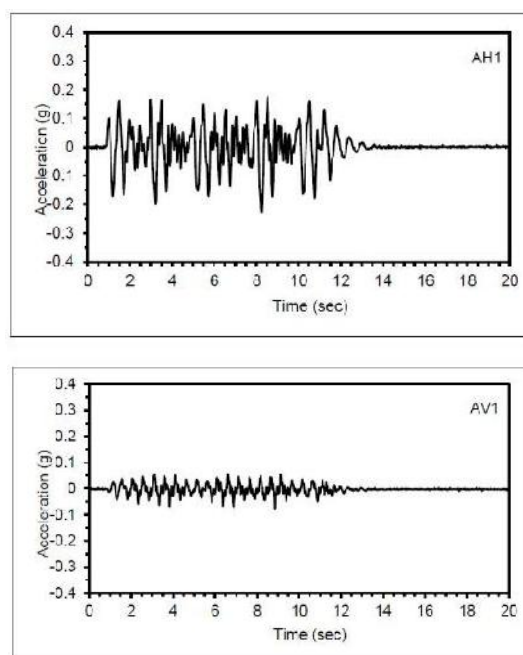


Figure 2. Input acceleration time history (horizontal and vertical)

## RESULTS

Figure 3 demonstrates excess pore pressures at location of p1, p2, p3 and p4 (at elevation 8.5, 7.5, 5 and 2.5 m). Comparison between numerical results and experimental observations indicates that numerical model is capable of predicting the excess pore pressure.

The accuracy of the numerical modelling to predict pore water pressure up to 20 second which is the end of dynamic loading is reasonable. However after 20 seconds the simulation shows a discrepancy with experimental results. The reason of this difference is due to the assumption of constant permeability coefficient; however this coefficient was changing in the loading procedure. Figure 4 displays lateral displacements at 2.5, 5, 7.5 and 10m elevations.



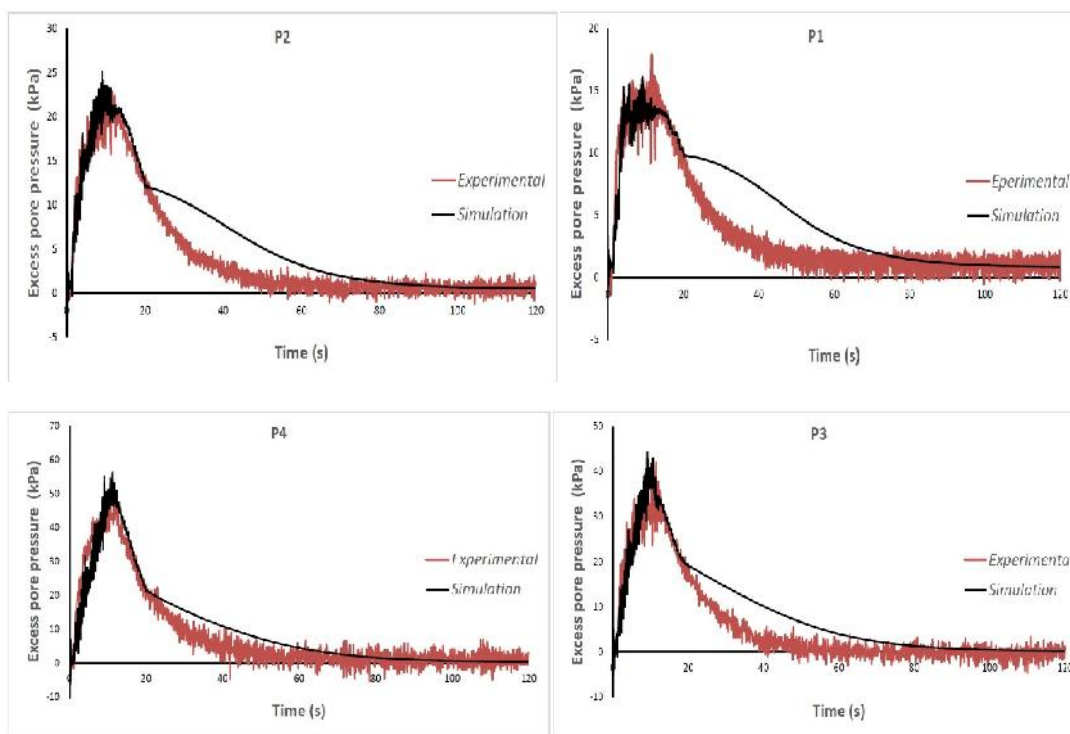


Figure3. Comparison of excess pore pressure between experimental and simulation in different elevation

Based on the obtained results, numerical model has good ability to predict maximum lateral displacements. Only at elevation 2.5m (LVDT 4) there is a difference between simulation and experimental results. However, considering LVDT 3 result, it is concluded that LVDT 4 experimental result is doubtful, and it seems numerical results are more accurate.

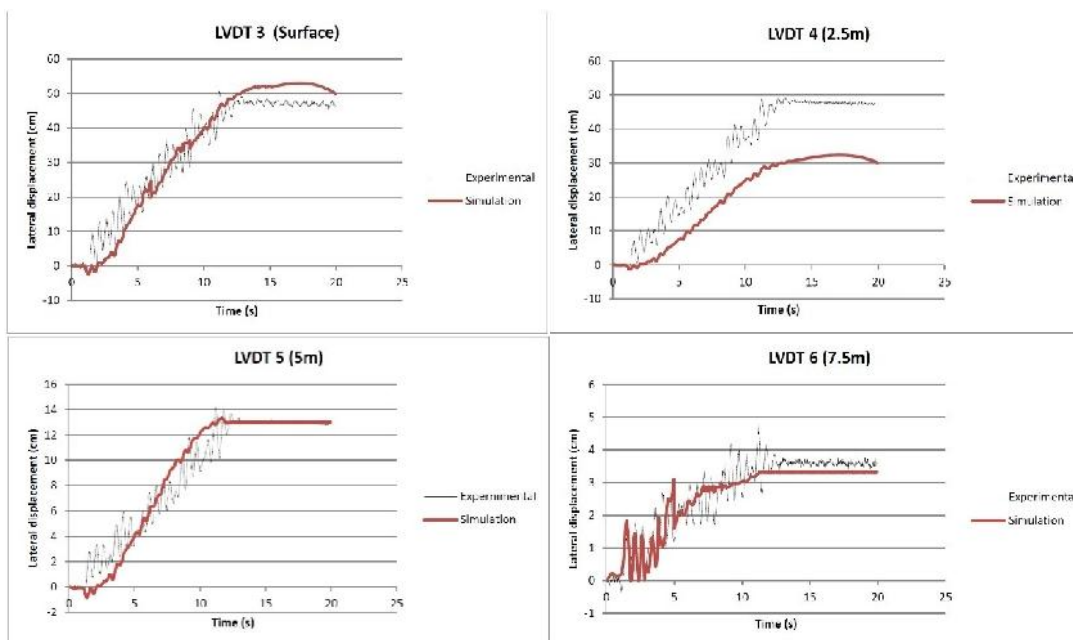


Figure4. Comparison of lateral displacements between experimental and simulation in different elevation

## INVESTIGATION OF FREQUENCY EFFECTS ON LATERAL DISPLACEMENT

The numerical methodology described in the previous section was used parametrically in order to study the effects of input frequencies. Five non-linear fully coupled effective stress analyses were performed followed the same simulation principles used for the analysis of the centrifuge experiment. However, in

this analysis the dynamic loading have been applied with a sinusoidal acceleration time history consists of five different frequencies. Table 4 gives the parameter used in the analysis.

Table 4. Parameters of analysis (geometry and loading)

Thickness of the liquefiable layer	Ground inclination	Maximum acceleration	Number of loading cycle	Frequency of loading
10 m	2°	0.15g	20	1,2,3,5,7,10 Hz

## 1. MAXIMUM LATERAL DISPLACEMENT

The amount of maximum displacement is significantly decreased by increasing the magnitude of frequency. The lateral displacements at ground surface are depicted in Figure 5. The reason of this reduction could be justified as the amplitude of input acceleration is constant, in the other hand input frequency is increased. So, soil displacements amplitude is reduced and ground vibrate with low amplitude. This event causes reduction in excess pore pressure generation rate. As shown in Figure 5, in smaller frequencies there is more vibration and when frequency is increased, these vibrations would have been reduced whenas the rate of loading has been increased.

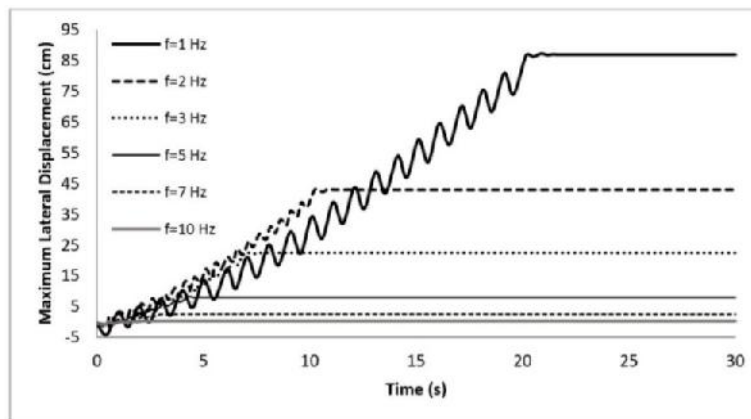


Figure 5. Variations of maximum lateral displacement with different frequencies

Figure 6 illustrates lateral displacements versus depth. The frequency has great impact on lateral displacement at various elevation, e.g. with frequency increase from 1Hz to 3Hz, lateral displacement at ground surface is reduced 74% and at 5m elevation is decreased 83%.

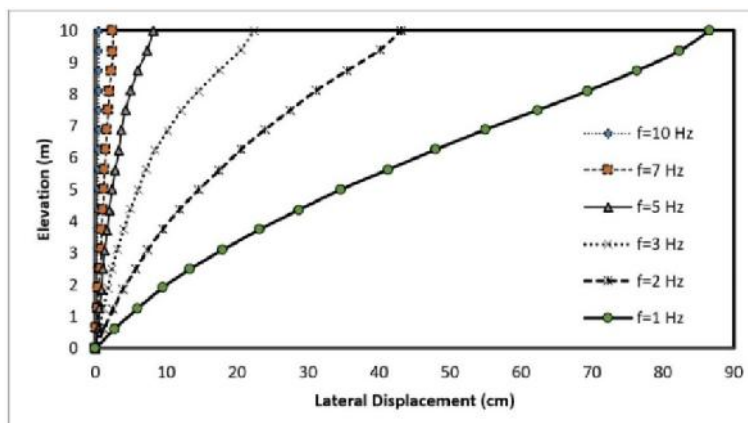


Figure 6. Variations of lateral displacement with different frequencies in depth

Figure 7 demonstrates normalized lateral displacements. At frequency 7 and 10Hz, due to great reduction in lateral displacement than other frequencies, tendency of normalized displacements are different. Actually, it seems that liquefaction did not occur at these frequencies.



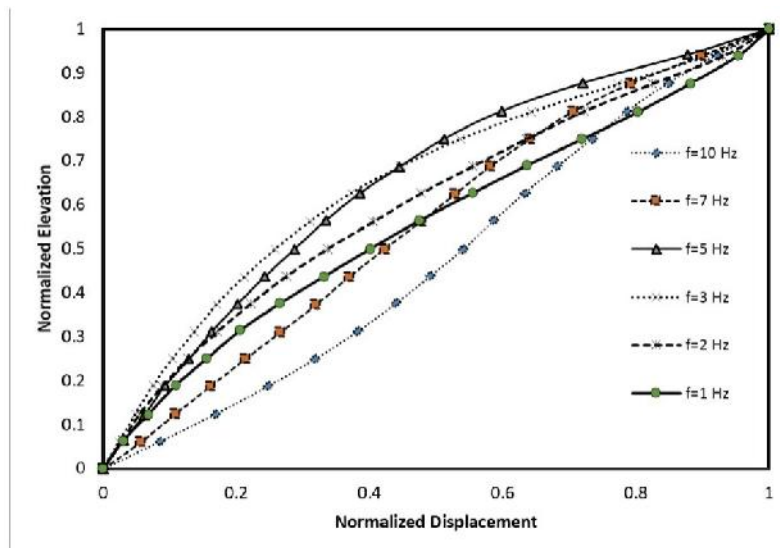


Figure 7. Variations of normalized lateral displacement with different frequencies in depth

## CONCLUSIONS

In this research, lateral spreading induced by liquefaction is simulated. For verification, simulation is compared against VELACS M2-1 centrifuge experiment. After validating, the effect of frequency of input motion is investigated. The results indicate that amount of displacement is significantly reduced by increasing the magnitude of frequency. According to the results, all of the displacements are occurred in the loading time and after the loading process, there is no additional lateral displacement.

## ACKNOWLEDGEMENTS

The authors would like to thank Prof. Andrew Chan of Federation University (Australia) for providing the computer code (GLADYS-2E) and his invaluable comments and guidance.

## REFERENCES

- Arulanandan K and Scott RF(1993) *Verification of Numerical Procedures for the Analysis of Soil Liquefaction Problems, Technical papers and discussions*, Vol. 2, Taylor & Francis
- Biot MA (1955) Theory of elasticity and consolidation for a porous anisotropic solid,*Journal of applied physics*, 26(2), 182-185
- Biot MA (1956) Theory of propagation of elastic waves in a fluid saturated porous solid. II. Higher frequency range,*The Journal of the Acoustical Society of America*, 28, 179
- Chan A, Famiyesin B, Madabhushi S and Wood D (1994) *Dynamic analyses of saturated soils: Comparison of implicit up and explicit uw formulations and the effect of initial conditions*, Paper presented at the Proc. XIII Intl. Conf. on Soil Mechanics and Foundation Engineering
- Chan A, Famiyesin O and Muir Wood D (1992) User Manual for GLADYS-2E,*Department of Civil Engineering, Glasgow University*
- Chan A and Zienkiewicz O (1998) *Numerical modelling of static and dynamic geomechanics problems using the generalised Biot formulation and comparison with centrifuge experiments*, Paper presented at the Proceedings of the Biot Conference on Poromechanics
- Chan AHC (1988) *A unified finite element solution to static and dynamic problems of geomechanics*,



University College of Swansea

Newmark NM (1959) *A method of computation for structural dynamics*, Paper presented at the Proc. ASCE

Pastor M, Zienkiewicz O and Chan A (1990) Generalized plasticity and the modelling of soil behaviour, *International Journal for Numerical and Analytical Methods in Geomechanics*, 14(3): 151-190

Taslimian R, Noorzad A and Noorzad A (2012) *Modeling saturated porous media with elasto-plastic behavior and non-Darcy flow law considering different permeability coefficients*, Paper presented at the proceedings of the 15th world conference on earthquake engineering, Lisbon, Portugal

Zienkiewicz O, Leung K and Pastor M (1985) Simple model for transient soil loading in earthquake analysis, I. Basic model and its application, *International Journal for Numerical and Analytical Methods in Geomechanics*, 9(5): 453-476

Zienkiewicz O and Shiomi T (1984) Dynamic behaviour of saturated porous media; the generalized Biot formulation and its numerical solution, *International Journal for Numerical and Analytical Methods in Geomechanics*, 8(1): 71-96

Zienkiewicz OC, Chan A, Pastor M, Schrefler B and Shiomi T (1999) *Computational geomechanics with special reference to earthquake engineering*, Wiley, Chichester